sciences Corp., NJ, USA) using Mini Trans-Blot Cell and Power/Pac 200 (Bio-Rad Laboratories Inc., CA, USA). Membranes were incubated with a 1:1000 dilution of human SXR antiserum (PXR, Santa Cruz Biotechnology, Inc., CA, USA) for overnight at 4 °C and a 1:1000 dilution of anti-goat IgG horseradish peroxidase (ICN Biomedicals, Inc., CA, USA) conjugated for one hour at room temperature. Protein bands were detected using the ECL Plus Western blotting detection reagent (Amersham Biosciences Corp.) and visualized with Las-1000 cooled CCD-camera chemiluminescent image analyzer (Fuji Photo Film Co., Ltd., Tokyo, Japan). The relative signal abundance was subsequently quantified as optical density (OD) value with Science Lab 99 Image Gauge 3.2 software (Fuji Photo Film Co., Ltd.). The intensity for SXR immunoreactivity was expressed as relative OD (arbitrary units).

2.4. Statistical analysis

Results were expressed as mean ± S.D. Statistical analysis was performed with the StatView 5.0 J software (SAS Institute Inc., NC, USA). All data were analyzed by analysis of variance (ANOVA) followed by post-hoc Bonferroni/Dunn multiple comparison test. A p-value < 0.05 was considered to indicate statistical significance.

3. Results

3.1. Systemic distribution of SXR, CYP3A and MDR1 in human adult and fetal tissues

Results of semi-quantitative analysis of SXR, CYP3A and MDR1 in adult (male, 54 and 24 years old; female, 38 and 15 years old) and fetal (male, 18, 19, and 21 weeks old; female, 20 and 21 weeks old) human tissues are summarized in Table 3. Data are expressed relative to GAPDH mRNA levels in each specimen. Expression of SXR mRNA was detected in adult liver, kidney, and small/large intestine, but was below the limits of detection in other tissues examined. SXR mRNA transcripts in fetal tissues were limited to liver, kidney, and small/large intestine.

CYP3A4 mRNA was detected in adult lung, esophagus, stomach, small/large intestine, adrenal gland, testis, and prostate (28.3–112.7% of adult liver expression). In those fetal tissues where CYP3A4 expression was detected, the mRNA levels were comparable with those in adult tissues (lung, small/large intestine, liver, and adrenal gland 22.1–64.7%). Relatively low levels of CYP3A4 mRNA were detected in adult pancreas, fetal brain, spleen, kidney, thyroid, and testis (2.5–19.1%). CYP3A4 mRNA was also detected in placenta and umbilical cord (63.5 and 0.00%,
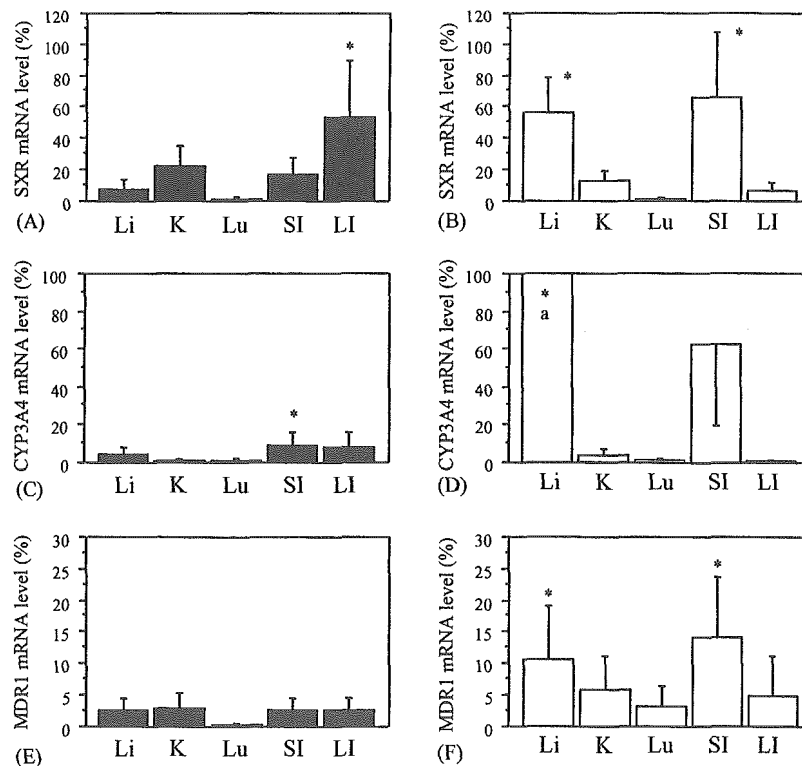

Fig. 1. Levels of mRNA for SXR, CYP3A4, and MDR1 in human fetal and adult tissues. (A) SXR mRNA levels in fetal tissues (*p < 0.05 vs. Li, K, Lu, and SI). (B) SXR mRNA levels in adult tissues (*p < 0.05 vs. K, Lu, and LI). (C) CYP3A4 mRNA levels in fetal tissues (*p < 0.05 vs. K and Lu). (D) CYP3A4 mRNA levels in adult tissues (*p < 0.05 vs. K, Lu, SI, and LI; a, 224 ± 61.9). (E) MDR1 mRNA levels in fetal tissues (there were no correlations among tissues examined). (F) MDR1 mRNA levels in adult tissues (*p < 0.05 vs. K, Lu, and LI). The number of each subjects was summarized as follows—Adult tissues: liver (Li), n = 24; kidney (K), n = 24; lung (Lu), n = 24; small intestine (SI), n = 16; large intestine (LI), n = 16. Fetal tissues: Li, n = 8; K, n = 8; Lu, n = 8; SI, n = 5; LI, n = 5. The data are expressed as the mean ± S.D.

respectively). MDR1 mRNA expression was detected in nearly all the tissues examined with levels ranging from 11–82% of adult SXR liver levels (adult tissues) and 11–87% (fetal tissues).

3.2. Age and sex differences

The highest levels of SXR mRNA expression were detected in adult liver and small intestine, fetal small/large intestine with lower levels in the adult/fetal lung and fetal liver (Fig. 1A and B). The levels of CYP3A4 mRNA expression were also higher in adult liver and small intestine than other tissues examined (Fig. 1C and D). CYP3A4 mRNA levels were relatively low in fetal tissues including liver and small intestines (Fig. 1C). MDR1 mRNA expression was similar to that of CYP3A4 mRNA in the tissues where they were co-expressed with the highest levels in the adult liver and small intestine (Fig. 1E and F).

There were no significant differences detected between male and female subjects in any of the adult human tissues examined (data not shown).

3.2.1. SXR

SXR mRNA expression was low in fetal and neonatal livers. Its levels subsequently increased in the young to middle

age group and then decreased to fetal levels in the elderly group (Fig. 2A). In kidney, the levels of SXR mRNA expression were relatively high in the fetus, but decreased towards term (Fig. 2B). In lung, SXR mRNA levels remained relatively low but variable throughout life (Fig. 2C). High levels of SXR mRNA expression were detected in the small intestine of the young-middle group (Fig. 2D). In the large intestine, SXR mRNA was expressed at high levels in the fetal group and then decreased to lower levels after birth (Fig. 2E).

3.2.2. CYP3A4

In liver, CYP3A4 mRNA expression was also low in the fetus up to neonatal group. In the young group, the levels of CYP3A4 mRNA transcripts markedly varied but were in general higher than those in the middle group (Fig. 3A). In kidney, the levels of CYP3A4 mRNA expression were highly variable within and across age groups of the subjects examined (Fig. 3B). As with SXR, CYP3A4 of lung was expressed at relatively low levels (Fig. 3C). High levels of CYP3A4 mRNA were also detected in the young group small intestine (Fig. 3D). As with SXR, CYP3A4 mRNA was only expressed at high levels in the fetal large intestine (Fig. 3E).

3.2.3. MDR1

MDR1 mRNA expression was relatively high in the elderly group liver, but the differences were not statistically
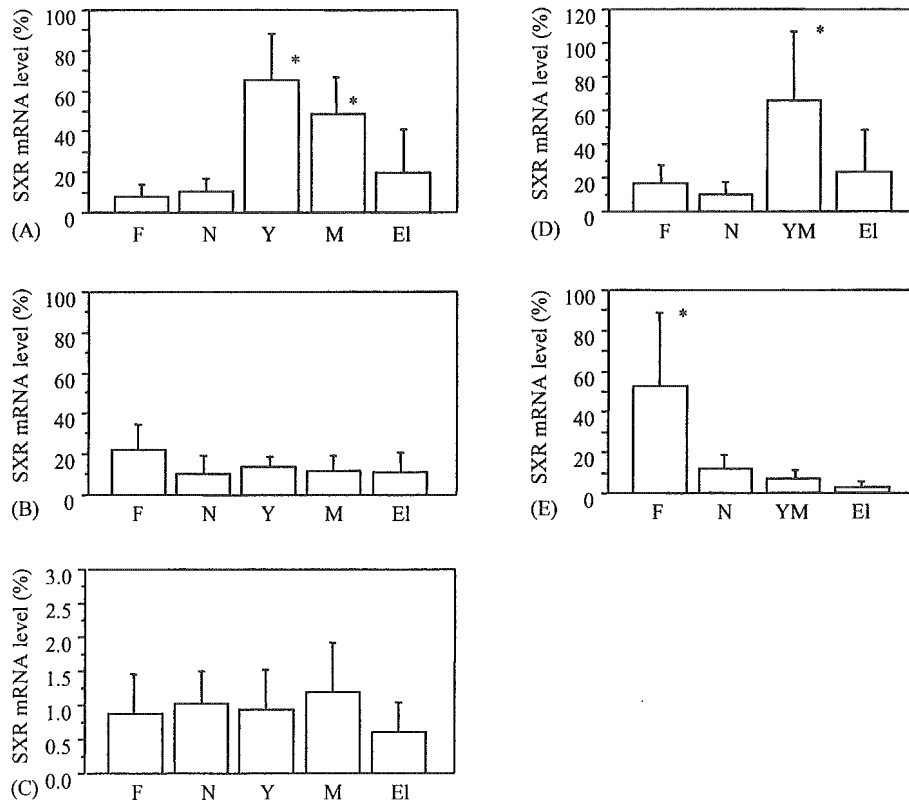

Fig. 2. Changes in SXR mRNA levels in human adult and fetal tissues through development and aging. (A) In liver ($^*p < 0.05$ vs. F, N, and El groups); (B) in kidney (no development and aging affected SXR mRNA levels); (C) in lung (no development and aging affected SXR mRNA levels); (D) in small intestine ($^*p < 0.05$ vs. N group); (E) in large intestine ($^*p < 0.05$ vs. N, YM, and El groups); (F) fetal. N, neonatal; Y, young; M, middle; El, elderly; YM, young-middle. The numbers of each subject are summarized in Table 1b. The data are expressed as the mean ± S.D.
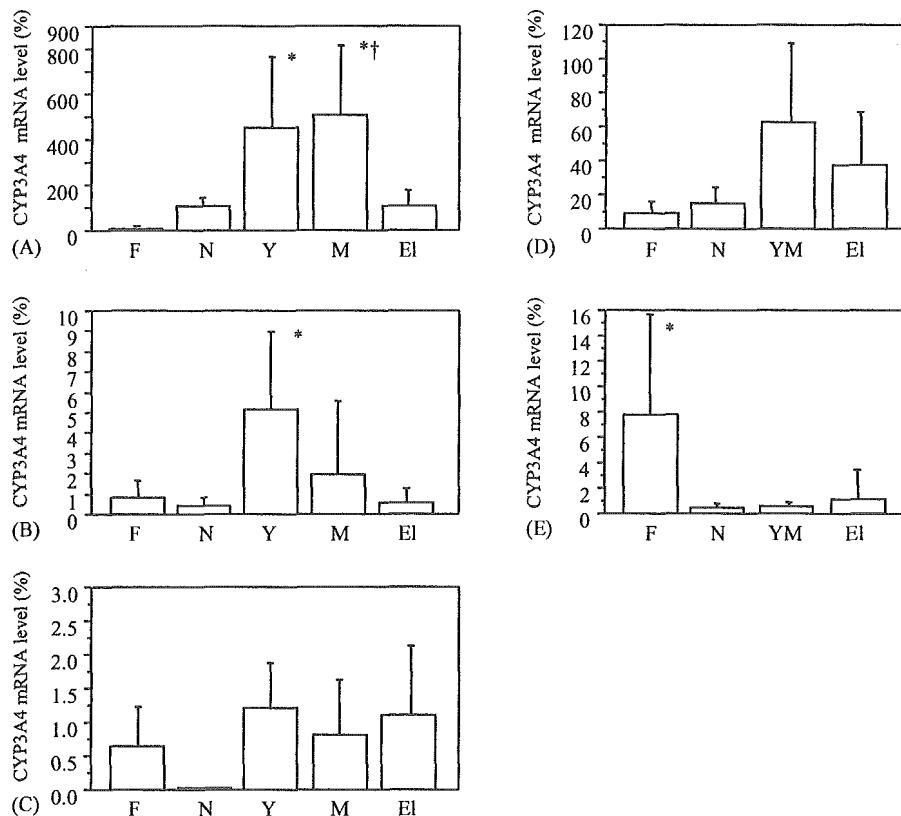
Fig. 3. Changes in CYP3A4 mRNA levels of human adult and fetal tissues through development and aging. (A) In liver ($^*p < 0.05$ vs. F and E groups; $^†p < 0.05$ vs. N group); (B) in kidney ($^*p < 0.05$ vs. F and E groups); (C) in lung (no development and aging affected CYP3A4 mRNA levels); (D) in small intestine (no development and aging affected CYP3A4 mRNA levels); (E) in large intestine ($^*p < 0.05$ vs. N, YM, and El groups); (F) fetal. N, neonatal; Y, young; M, middle; El, elderly; YM, young-middle. The numbers of each subject are summarized in Table 1b. The data are expressed as the mean ± S.D.

significant. In the neonatal group liver, MDR1 expression was relatively low but it increased with development and reached a plateau in the young group liver (Fig. 4A). The levels of MDR1 mRNA expression in kidney were low in fetus to neonatal group and later increased and remained relatively constant with maximal expression in the young group (Fig. 4B). In lung, MDR1 mRNA expression was very low in fetus but increased with development, and reached plateau in the young group and decreased thereafter (Fig. 4C). MDR1 expression levels were relatively low in both small and large intestine (Fig. 4D and E) throughout life with the exception of the small intestine in the young group.

3.3. Microdissection/PCR

Results of combined LCM/RT-PCR analysis of SXR, CYP3A4, and MDR1 in human kidney and small intestine are summarized in Table 4 and Fig. 5.

In adult human kidney, SXR PCR products were detected as a specific single band in whole kidney tissues and in urinary tubular epithelial cells isolated by LCM. SXR mRNA was reproducibly absent from the adult glomerulus whereas low levels of SXR mRNA expression were detected in stromal cells from one of three adult cases examined in our study (55

years old). CYP3A4 and MDR1 mRNAs were also detected in urinary tubular epithelial cells but not in the glomeruli. Low levels of CYP3A4 mRNA expression were also detected in stromal cells from one of three adults (55 years old), that also expressed SXR at low levels in these cells. SXR and CYP3A4 mRNAs were detected in urinary tubules and surrounding stromal cells in fetal kidney examined. MDR1 mRNA transcripts were detected only in the adult and fetal urinary tubules.

In adult small intestine, SXR and CYP3A4 mRNA expression were detected in surface epithelial cells, but not in tela submucosa and tunica muscularis. We could examine only one subject, but SXR and CYP3A4 mRNA expression were both detected in lamina propria mucosae of this 57-year-old male. MDR1 mRNA expression was restricted to surface epithelial cells. In the fetal small intestine, both SXR and CYP3A4 mRNA expression were detected in surface epithelial cells, but not in tunica muscularis. SXR and CYP3A4 mRNA were detected in the tela submucosa of fetal small intestine. MDR1 mRNA transcripts were restricted to surface epithelial cells as in the adult. Expression of GAPDH was detected in all the specimens examined in this combined LCM/RT-PCR analysis.
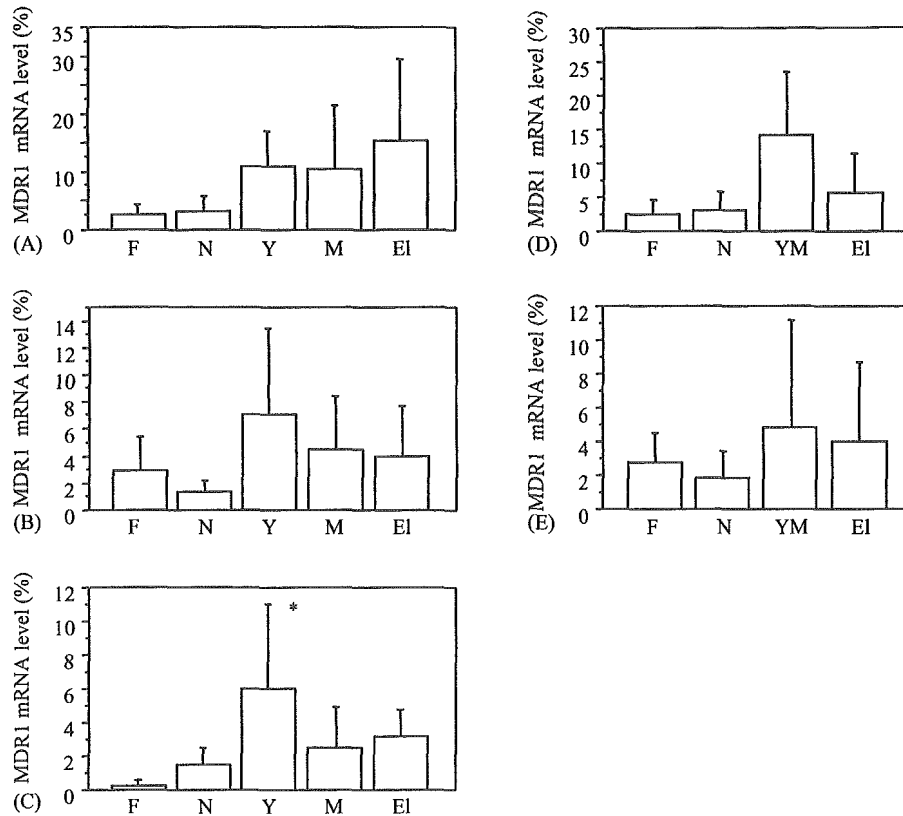
Fig. 4. Changes of MDR1 mRNA levels in human adult and fetal tissues through development and aging. There were no correlations between development and aging in MDR1 mRNA levels of liver (A), kidney (B), small intestine (D), and large intestine (E). In lung (C), a statistically significant difference was detected ($^*p < 0.05$ vs. N, YM, and El groups). F, fetal; N, neonatal; Y, young; M, middle; El, elderly; YM, young-middle. The numbers of each subject are summarized in Table 1b. The data are expressed as the mean ± S.D.

3.4. Immunoblotting analysis

Immunoblotting analysis demonstrated that expression of SXR protein (approximately 52 kDa) was detected in human liver, kidney, lung, small intestine, and large intestine, but was below the limits of detection in spleen and stomach (Fig. 6A). The highest levels of SXR immunoreactivity were detected in liver and small intestine with relatively lower levels in kidney. Weak immunoreactivity was detected in lung and large intestine. In spleen and stomach, SXR immunoreactivity was not detected [Fig. 6B (left)]. SXR protein expression was low in the fetal and 0-year-old liver, whereas high levels of SXR protein expression were detected in adult liver [Fig. 6C (left)]. Results of SXR immunoreactivity were consistent with those of SXR mRNA transcripts [Fig. 6B (right) and C (right)].

4. Discussion

SXR expression has been reported in human adult liver, small intestine, and large intestine by several groups of investigators (Bertilsson et al., 1998; Blumberg et al., 1998a; Lehmann et al., 1998). Our results were consistent with these results, but in this study we also detected SXR expression

in adult lung and kidney. In human liver, the levels of SXR, CYP3A4, and MDR1 mRNAs were all detected in both fetus and neonates. CYP3A7 was the major CYP3A form in fetal liver, and Hakkola et al. (2001) demonstrated that the abundance of CYP3A7 varied more markedly at the mRNA levels than at the protein level. CYP3A5 mRNA has been also reported in fetal liver, but the average level was 700-fold lower than that of CYP3A7 (Hakkola et al., 2001). In addition, CYP3A5 mRNA was detected only in a subset of the fetal liver specimens and its level was the lowest among CYP3A forms (Hakkola et al., 2001).

Bertilsson et al. (1998) demonstrated that in 10-week human embryos, expression was limited to the intestinal mucosal layer using in situ hybridization analysis. In our present LCM analysis, SXR mRNA was also detected in tela submucosa of fetal small intestine. In this study, we could also detect CYP3A4 and MDR1 mRNA transcripts in the adult and fetal intestinal epithelium. It is well known that the small intestine is one of the most important organs for the metabolism and clearance of both endogenous and exogenous substrates including steroids. This is consistent with the findings of our present study in that SXR, CYP3A4, and MDR1 mRNA transcripts were markedly present in adult and fetal small intestine. SXR and CYP3A4 mRNAs were also abundantly ex-

Table 4
Summary of laser capture microdissection/RT-PCR in human kidney and small intestine

	No.	Age	Sex	Kidney			Small intestine			
				G	T	S	E	PM	SM	M
SXR										
Adult	1	17	M	0	2	0				
	2	55	M	0	3	1				
	3	38	F	0	2	0				
	4	57	M				3	1	0	0
	5	76	M				3	a	0	0
Fetus	6	21	M	0	1	2	3	a	1	0
	7	21	F	0	1	2	3	a	1	0
CYP3A4										
Adult	1	17	M	0	2	0				
	2	55	M	0	1	1				
	3	38	F	0	3	0				
	4	57	M				3	1	0	0
	5	76	M				3	a	0	0
Fetus	6	21	M	0	1	1	2	a	1	0
	7	21	F	0	1	1	2	a	1	0
MDR1										
Adult	1	17	M	0	1	0				
	2	55	M	0	2	0				
	3	38	F	0	2	0				
	4	57	M				3	0	0	0
	5	76	M				3	a	0	0
Fetus	6	21	M	0	1	0	1	a	0	0
	7	21	F	0	1	0	1	a	0	0

M, male; F, female; 0, negative; 1, weak; 2, moderate; 3, strong; G, glomerulus; T, urinary tubules; S, stromal cells; E, epithelium; PM, lamina propria; SM, tela submucosa; M, tunica muscularis. In kidney, adult, $n = 3$; fetus, $n = 2$. In small intestine, adult, $n = 2$; fetus, $n = 2$.
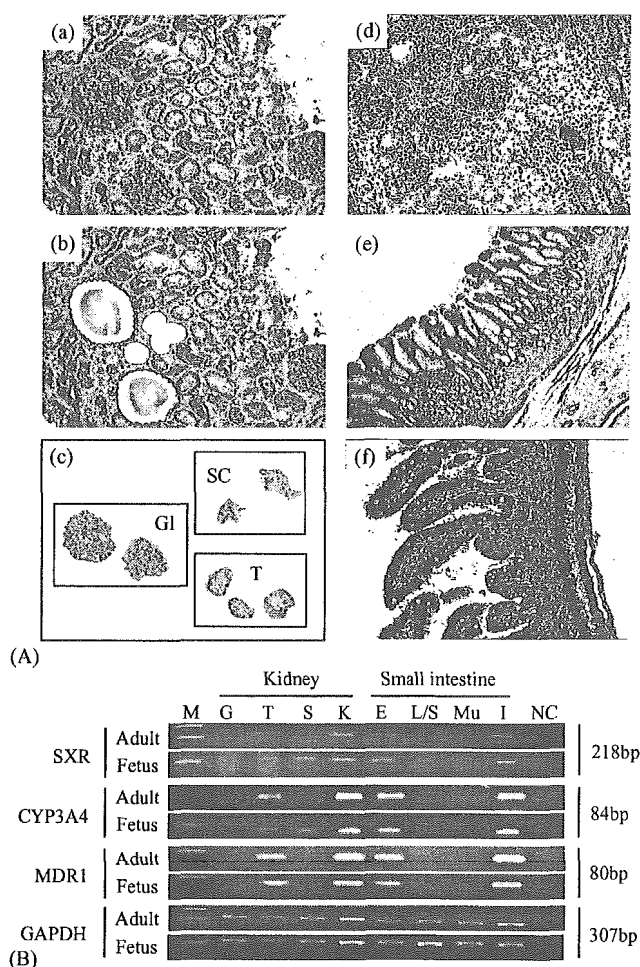
[a] No specimens were available for study.

Fig. 5. (A) Toluidine blue staining for laser capture microdissection (LCM) in human kidney and small intestine. The numbers of each subject are summarized in Table 1b: (a) human adult kidney; (b) after microdissection; (c) after laser pressure cell transfer (Gl, glomerulus; T, tubules; SC, stromal cells); (d) human fetal kidney; (e) human adult small intestine; (f) human fetal small intestine. (B) Results of electrophoresis of microdissection/RT-PCR. Results are summarized in Table 4. In adult kidney, mRNA expression for SXR, CYP3A4, and MDR were detected only in urinary tubules. In fetal kidney, mRNA expressions for SXR, CYP3A4, were detected in urinary tubules and stromal cells. MDR1 mRNA expression was detected only in urinary tubules. In adult small intestine, mRNA expression for SXR, CYP3A4, were detected in epithelium, and lamina propria mucosae (data not shown), and tunica muscularis in this case. MDR1 expression was detected only in surface epithelium. In fetal small intestine, mRNA expression for SXR, CYP3A4, were detected in epithelium, and tela submucosa. In all cases, GAPDH was detected as a specific single band. G, glomerulus; T, urinary tubules; S, stromal cells surrounding the urinary tubules; K, whole tissue of same kidney; E, epithelium; L, lamina propria mucosae of adult; S, tela submucosa of fetus; M, tunica muscularis; I, whole tissue of same small intestine; N.C., negative control; M, 100 bp ladder.

pressed in the fetal large intestine. The ability to absorb or digest nutrients is generally considered to be acquired from fetus to newborn in the small and large intestine (Babyatsky and Podolsky, 1999). In adult kidney, SXR mRNA transcripts were detected only in the urinary tubules whereas SXR transcripts were also detected in interstitial and stromal cells surrounding the urinary tubules in fetal kidney. CYP3A4 mRNA expression was considered dominant in adult urinary tubules, whereas it was dominant in the stromal cells of the fetal kidney. The possible roles of SXR and CYP3A4 in the fetal kidney may include an inactivation of steroids and xenobiotics, possibly leaking from the urinary tubules due to their immaturity.

It is known that the liver function, including xenobiotic metabolism decreases with aging. Moreover, neonatal liver is known to be immature in its ability to metabolize compounds (Greenblatt et al., 1982; Wynne et al., 1989; Sotaniemi et al., 1997; de Wildt et al., 1999). Our study suggests that SXR levels are at least partly responsible for these reductions in drug clearance in elderly subjects, but this also requires further investigations for confirmation. Individual differences

in the CYP enzymatic activities decrease with aging (Hunt et al., 1992). However, the differences of the amounts of CYPs detected in each age group examined were lower than expected in our study. Masuyama et al. (2003) reported that SXR was not detected in normal endometrium but was expressed in the endometrium of patients who took oral
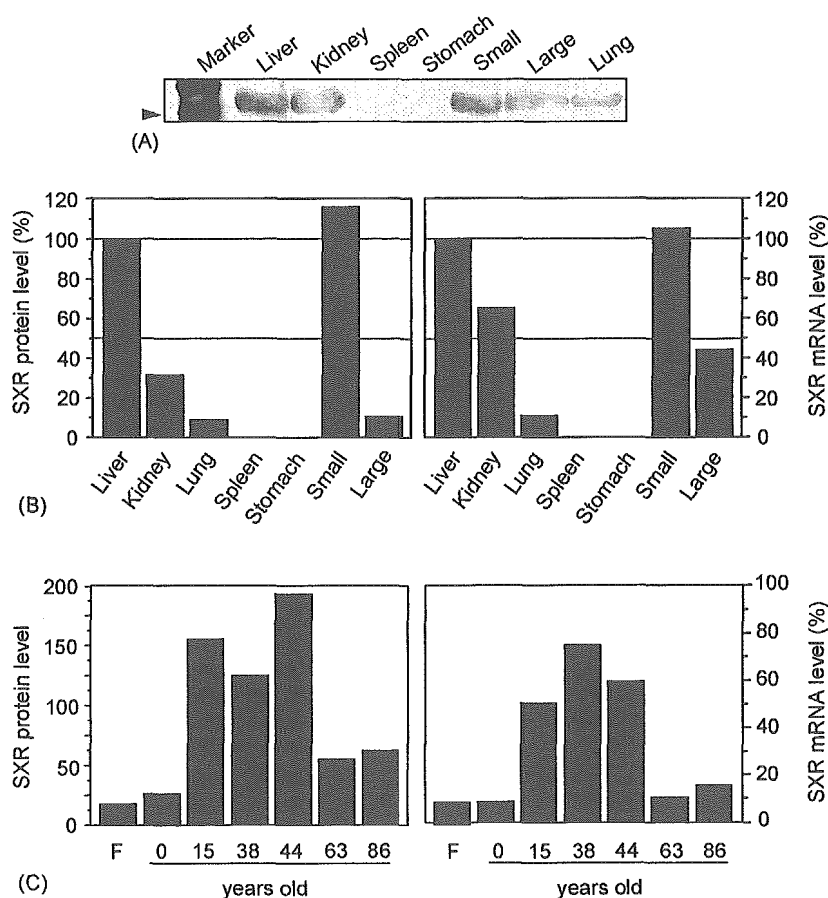
Fig. 6. Results of immunoblotting analysis for SXR in human tissues. (A) Expression of protein for SXR was detected in adult (38-year-old women) liver, kidney, lung, small intestine, and large intestine (arrow head, 50 kDa). (B) The levels of SXR immunoreactivity were high in liver, kidney, and small intestine, low in lung and large intestine (left panel). SXR mRNA transcripts (right panel) were also detected in liver, kidney, lung, small intestine, and large intestine. (C) The levels of SXR protein and mRNA transcripts in adult and fetal livers. SXR protein expression was low in the fetal and 0-year-old livers, whereas the high levels of SXR protein expression were detected in adult livers (left panel). As with SXR protein expression patterns, SXR mRNA transcripts (right panel) were high in 15–44 years old, and low in fetus, 0, 63, and 86 years old. Small, small intestine; Large, large intestine; Marker, size marker. The numbers of each subject are summarized in Table 1b.

contraceptives. Masuyama et al. (2001) also reported the expression of PXR mRNA in reproductive organs such as the ovary, uterus, and placenta of non-pregnant and/or pregnant mice. These authors suggested that the steroid strongly influences SXR expression in human endometrium and rodent reproductive organs. Aging and/or maturation are associated with concomitant change in activities of steroid hormones in both male and female (Beitins et al., 1973; Hermann et al., 2000; Purohit and Reed, 2002). In addition, SXR transcripts have been reported from both normal breast tissue and breast carcinoma (Dotzlaw et al., 1999). Estradiol has traditionally been considered to play a critical role in female reproductive organs, normal breast, and breast cancer and is well known to activate SXR-dependent transcription (Blumberg et al., 1998a) and to be metabolized by CYP3A4 (Lee et al., 2001). These reported findings, taken together with the results presented above indicated that changes in SXR levels associated with the aging/maturation process may be related to physiological responses in the response to steroid and xenobiotic exposure.

Acknowledgments

References

Anttila, S., Hukkanen, J., Hakkola, J., Stjernvall, T., Beaune, P., Edwards, R.J., Boobis, A.R., Pelkonen, O., Raunio, H., 1997. Expression and localization of CYP3A4 and CYP3A5 in human lung. Am. J. Respir. Cell Mol. Biol. 16, 242–249.

Babyatsky, M.W., Podolsky, D.K., 1999. Growth and development of the gastrointestinal tract. In: Yamada, T. (Ed.), Textbook of Gastroen-

terology, 3rd ed. Liptoncott Williams and Wilkins, Philadelphia, pp. 547–584.

Beitins, I.Z., Bayard, F., Ances, I.G., Kowarski, A., Migeon, C.J., 1973. The metabolic clearance rate, blood production, interconversion and transplacental passage of cortisol and cortisone in pregnancy near term. Pediatr. Res. 7, 509–519.

Bertilsson, G., Heidrich, J., Svensson, K., Åsman, M., Jendeberg, L., Sydow-Bäckman, M., Ohlsson, R., Postlind, H., Blomquist, P., Berkenstam, A., 1998. Identification of a human nuclear receptor defines a new signaling pathway for CYP3A induction. Proc. Natl. Acad. Sci. U.S.A. 95, 12208–12213.

Blumberg, B., Sabbagh Jr., W., Juguilon, H., Bolado Jr., J., van Meter, C.M., Ong, E.S., Evans, R.M., 1998a. SXR, a novel steroid and xenobiotic-sensing nuclear receptor. Gene Dev. 12, 3195–3205.

Blumberg, B., Kang, J., Bolado Jr., J., Chen, H., Craig, A.G., Moreno, T.A., Umesono, K., Parlmann, T., De Robertis, E.M., Evans, R.M., 1998b. BXR, an embryonic orphan nuclear receptor activated by novel class of endogenous benzoate metabolites. Gene Dev. 12, 1269–1277.

Cordon-Cardo, C., O'Brien, J.P., Boccia, J., Casals, D., Bertino, J.R., Melamed, M.R., 1990. Expression of the multidrug resistance gene product (P-glycoprotein) in human normal and tumor tissues. J. Histochem. Cytochem. 38, 1277–1287.

de Wildt, S.N., Kearns, G.L., Leeder, J.S., van den Anker, J.N., 1999. Cytochrome P450 3A: ontogeny and drug disposition. Clin. Pharmacokinet. 37, 485–505.

Domanski, T.L., Finta, C., Halpert, J.R., Zaphiropoulos, P.G., 2001. cDNA cloning and initial characterization of CYP3A43, a novel human cytochrome P450. Mol. Pharmacol. 59, 386–392.

Dotzlaw, H., Leygue, E., Watson, P., Murphy, L.C., 1999. The human orphan receptor PXR messenger RNA is expressed in both normal and neoplastic breast tissue. Clin. Cancer Res. 5, 2103–2107.

Dussault, I., Forman, B.M., 2002. The nuclear receptor PXR: a master regulator of "homeland" defense. Crit. Rev. Eukaryot. Gene Exp. 12, 53–64.

Emmert-Buck, M.R., Bonner, R.F., Smith, P.D., Chuaqui, R.F., Zhuang, Z., Goldstein, S.R., Weiss, R.A., Liotta, L.A., 1996. Laser capture microdissection. Science 274, 998–1001.

Faneyte, I.F., Kristel, P., van de Vijver, M.J., 2001. Determining MDR/P-glycoprotein expression in breast cancer. Int. J. Cancer 93, 114–122.

Geick, A., Eichelbaum, M., Burk, O., 2001. Nuclear receptor response elements mediate induction of intestinal MDR1 by rifampin. J. Biol. Chem. 276, 14581–14587.

Gellner, K., Eiselt, R., Hustert, E., Arnold, H., Koch, I., Haberl, M., Deglmann, C.J., Buck, O., Buntefuss, D., Escher, S., Bishop, C., Koebe, H.G., Brinkmann, U., Klenk, H.P., Kleine, K., Meyer, U.A., Wojnowski, L., 2001. Genomic organization of the human CYP3A locus: identification of a new, inducible CYP3A gene. Pharmacogenetics 11, 111–121.

Greenblatt, D.J., Sellers, E.M., Shader, R.I., 1982. Drug therapy: drug disposition in old age. New Engl. J. Med. 306, 1081–1088.

Hakkola, J., Raunino, H., Purkunen, R., Saarikoski, S., Vahakangas, K., Pelkonen, O., Edwards, R.J., Boobis, A.R., Pasanen, M., 2001. Cytochrome P450 3A expression in the human fetal liver: evidence that CYP3A5 is expressed in only a limited number of fetal livers. Biol. Neonate 80, 193–201.

Hermann, M., Untergasser, H., Rumpold, H., Berger, R.P., 2000. Aging of the male reproductive system. Exp. Gerontol. 35, 1267–1279.

Hunt, C.M., Westerkam, W.R., Stave, G.M., Wilson, J.A., 1992. Hepatic cytochrome P-4503A (CYP3A) activity in the elderly. Mech. Ageing Dev. 64, 189–199.

Kliewer, S.A., Goodwin, B., Willson, T.M., 2002. The nuclear pregnane X receptor: a key regulator of xenobiotic metabolism. Endocr. Rev. 23, 687–702.

Lee, A.J., Kosh, J.W., Conney, A.H., Zhu, B.T., 2001. Characterization of the NADPH-dependent metabolism of 17beta-estradiol to multiple metabolites by human liver microsomes and selectively expressed human cytochrome P450 3A4 and 3A5. J. Pharmacol. Exp. Ther. 298, 420–432.

Lehmann, J.M., McKee, D.D., Watson, M.A., Willson, T.M., Moor, J.T., Kliewer, S.A., 1998. The human orphan nuclear receptor PXR is activated by compounds that regulate CYP3A4 gene expression and cause drug interaction. J. Clin. Invest. 102, 1016–1023.

Masuyama, H., Hiramatsu, Y., Mizutani, Y., Inoshita, H., Kudo, T., 2001. The expression of pregnane X receptor and its target gene, cytochrome P450 3A1, in perinatal mouse. Mol. Cell Endocrinol. 172, 47–56.

Masuyama, H., Hiramatsu, Y., Kodama, J.-I., Kudo, T., 2003. Expression and potential roles of pregnane x receptor in endometrial cancer. J. Clin. Endcrinol. Metab. 88, 4446–4454.

Michalets, E.L., 1998. Update: clinically significant cytochrome P-450 drug interaction. Pharmacotherapy 18, 84–112.

Miki, Y., Nakata, T., Suzuki, T., Darnel, A.D., Moriya, T., Kaneko, C., Hidaka, K., Shiotsu, Y., Kusaka, H., Sasano, H., 2002. Systemic distribution of steroid sulfatase and estrogen sulfotransferase in human adult and fetal tissues. J. Clin. Endcrinol. Metab. 87, 5760–5768.

Miyoshi, Y., Ando, A., Takamura, Y., Taguchi, T., Tamaki, Y., Noguchi, S., 2002. Prediction of response to docetaxel by CYP3A4 mRNA expression in breast cancer tissues. Int. J. Cancer 97, 129–132.

Nelson, D.R., Koymans, L., Kamataki, T., Stegeman, J.J., Feyereisen, R., Waxman, D.J., Waterman, M.R., Gotoh, O., Coon, M.J., Estabrook, R.W., Gunsalus, I.C., Nebert, D.W., 1996. P450 superfamily: update on new sequences, gene mapping, accession numbers and nomenclature. Pharmacogenetics 6, 1–42.

Niino, Y., Irie, T., Takaishi, M., Hosono, T., Huh, N., Tachikawa, T., Kuroki, T., 2001. PKCθII, a new isoform of protein kinase C specifically expressed in the seminiferous tubules of mouse testis. J. Biol. Chem. 276, 36711–36717.

Osterheld, J.R., 1998. A review of developmental aspects of cytochrome P450. J. Child Adolesc. Psychopharmacol. 8, 161–174.

Purohit, A., Reed, M.J., 2002. Regulation of estrogen synthesis in postmenopausal women. Steroids 67, 979–983.

Sotaniemi, E.A., Arranto, A.J., Pelkonen, O., Pasanen, M., 1997. Age and cytochrome P450-linked drug metabolism in humans: an analysis of 226 subjects with equal histopathologic conditions. Clin. Pharmacol. Ther. 61, 331–339.

Synold, T.W., Dussault, I., Forman, B.M., 2001. The orphan nuclear receptor SXR coordinately regulates drug metabolism and efflux. Nat. Med. 7, 584–590.

Thiebaut, F., Tsuruo, T., Hamada, H., Gottesman, M.M., Pastan, I., Willingham, M.C., 1987. Cellular localization of the multidrug-resistance gene product P-glycoprotein in normal human tissues. Proc. Natl. Acad. Sci. U.S.A. 84, 7735–7738.

van Kalken, C., Giaccone, G., va der Valk, P., Kuiper, C.M., Hadisaputro, M.M., Bosma, S.A., Scheper, R.J., Meijer, C.J., Pinedo, H.M., 1992. Multidrug resistance gene (P-glycoprotein) expression in the human fetus. Am. J. Pathol. 141, 1063–1072.

Westlind, A., Malmebo, S., Johansson, I., Otter, C., Andersson, T.B., Ingelman-Sundberg, M., Oscarson, M., 2001. Cloning and tissue distribution of a novel human cytochrome p450 of the CYP3A subfamily, CYP3A43. Biochem. Biophys. Res. Commun. 281, 134–135.

Willson, T.M., Kliewer, S.A., 2002. PXR, CAR and drug metabolism. Nat. Rev. Drug Discov. 1, 259–266.

Wynne, H.A., Cope, L.H., Mutch, E., Rawlins, M.D., Woodhouse, K.W., James, O.F., 1989. The effect of age upon liver volume and apparent liver blood flow in healthy man. Hepatology 9, 297–301.

Xie, W., Evans, R.M., 2001. Orphan nuclear receptors: the exotics of xenobiotics. J. Biol. Chem. 276, 37739–37742.

CANCER
Letters

Analysis of gene expression induced by diethylstilbestrol (DES) in human primitive Müllerian duct cells using microarray

Yasuhiro Miki[a,*], Takashi Suzuki[a], Chika Tazawa[a], Masato Ishizuka[a], Shuho Semba[b], Itsuo Gorai[c], Hironobu Sasano[a]

[a]Department of Pathology, Tohoku University Graduate School of Medicine, 2-1 Seiryo-machi Aoba-ku, Sendai, Miyagi 980-8575, Japan
[b]Division of Surgical Pathology, Kobe University Graduate School of Medicine, Kobe, Hyogo 650-0017, Japan
[c]Department of Obstetrics and Gynecology, International University of Health and Welfare Atami Hospital, Atami, Shizuoka 413-0012, Japan

Abstract

The Müllerian ducts are strongly influenced by natural estrogen, estradiol (E2) and diethylstilbestrol (DES) in their development. We screened E2 and DES responsive genes using a microarray analysis in human primitive Müllerian duct cell line, EMTOKA cells expressed estrogen receptor (ER) β. c-*myc* oncogene and other target genes expression was detected in cells treated by high-dose DES, but ER antagonist ICI 182,780 could not prevent c-*myc* induction above. Results of our present study suggested the presence of ER independent pathway in oncogenes induction process by high-dose DES treatment in a human primitive Müllerian duct cell line.
© 2004 Elsevier Ireland Ltd. All rights reserved.

Keywords: Diethylstilbestrol (DES); Estradiol; Microarray; Müllerian duct cell; c-*myc*

1. Introduction

In 1940s, non-physiological estrogens including Diethylstilbestrol (DES) or DES-type drugs were commonly used in the USA for the treatment of high-risk pregnancies, and have been prescribed to more than five million pregnant women [1]. However, in 1953, it was Dieckmann et al. [2] who first cast doubts on the efficacy of DES in the treatment of

high-risk pregnancies. Furthermore, the possible association between treatment of DES during pregnancy and development of clear-cell adenocarcinoma of the vagina or cervix in so-called DES-daughters (woman whose mothers took DES while pregnant with them) has been proposed by several epidemiologist including DES-Adenosis Project in USA in 1970s–1980s [3,4].

Uterus and the upper vagina are well known to have a common origin, the Müllerian duct. In human, Müllerian ducts can be identified in embryos of both sexes at 6 weeks of gestation age. By the 9th weeks of gestation, Müllerian ducts elongated and reached the urogenital sinus. The two ducts fused and further

---

* Corresponding author. Tel: +81-22-717-8050; fax: +81-22-717-8051.
E-mail address: miki@patholo2.med.tohoku.ac.jp (Y. Miki).

proceeded from caudal to cephalic portions of the fetus up to the level of uterine fundus. Internal canalization and septum resorption occur by approximately 20 weeks of gestation [5]. Müllerian duct has also been well known to be strongly influenced by estrogenic compounds such as estradiol (E2) and DES, and to result in both functional and morphological changes of vagina following the birth. Marked association of E2, potential natural estrogen, or DES with female reproductive carcinogenicity has been well established in several animal models [6]. Biological activity of natural estrogen is mediated through an initial interaction with estrogen receptor α (ERα) or β (ERβ). Xenobiotic compounds including endocrine disrupters also bind to estrogen receptors and exert estrogenic effects in many tissues. DES can result in reproductive tract abnormalities of rodents including endometrial adenocarcinoma through disruption of endocrine systems [7].

In addition, possible effects of DES on both female and male fetal reproductive system have been well known for many years [3,4,8]. Especially recently, actions of DES have been postulated in the context of endocrine disrupting chemicals. A possible influence of DES on human development is very important, but it is also true that the study of DES induced anomalies has been largely limited to rodents, and in vitro toxicity analysis in human tissues and cells has not been reported. Furthermore, an association between development of clear-cell adenocarcinoma of vagina and in utero DES exposure has been clearly established, but its mechanism has not been established. Therefore, in this study, we employed human primitive Müllerian duct cell line, EMTOKA 5E4 clone (EMTOKA) cells, established from uterine carcinosarcoma obtained from the patient [9,10] as an initial attempt to evaluate these effects of DES on development of human reproductive systems. This cell line expressed ERβ mRNA transcript and protein. We first examined the effect of E2 or DES treatment in EMTOKA cells using cell proliferation assays. We then screened E2 and/or DES (high and low-dose) responsive genes using a microarray analysis in these cells. The expression of c-*myc* oncogene, which was considered one of the most important genes induced by DES as a result of microarray analysis, was further characterized using quantitative RT-PCR and immunoblotting in these

cell line. We subsequently evaluated whether an induction of c-*myc* mRNA transcripts by DES treatment was mediated using ER or not using ERα and β inhibitor, ICI 182,780 pre-treatment assay, in order to further characterize the possible effects of DES on EMTOKA cells.

2. Materials and methods

2.1. Chemicals

E2 (β-estradiol) and DES (diethylstilbestrol) were purchased from Sigma-Aldrich Co. (MO, USA). ICI 182,780 (ICI) was purchased from Tocris Cookson Inc. (MO, USA). The test materials, E2 and DES were dissolved in ethanol (Wako Pure Chemical industries, Ltd, Osaka, Japan) and serially diluted (final concentrations: 10^{-12}–10^{-5} M), respectively. ICI was also dissolved in ethanol and diluted (final concentration: 10^{-6} M [11]). The final concentrations of ethanol used in this study did not exceed 0.05% in any of the cases examined.

2.2. Cell line and culture conditions

Primitive Müllerian duct cells, EMTOKA 5E4 clone cell line was established from uterine carcinosarcoma obtained from the patient [9,10]. The cell line was maintained in control RPMI-1640 medium (Sigma-Aldrich Co.) supplemented with 10% fetal bovine serum (FBS (JRH Biosciences, KS, USA)). Cells were maintained in culture at 37 °C, 95% relative humidity and 5% CO_2 in room air. The cells were pre-incubated for 24 h with serum-free medium prior to examination. The cells were harvested in serum-free medium and were plated on 6-well plates at initial concentration of 3×10^4 cells/ml. Different concentrations of test compounds were added, and the assay was terminated after 24, 48, and 72 h by removing the medium from wells, extracting total RNA using TRIzol method. For ICI pre-treatment [11], ICI was added 24 h before the additions of E2 or DES. MCF-7 employed in ICI inhibitory assay was obtained from Cell Resource Center for Biomedical Research, Institute of Development, Aging and Cancer, Tohoku University (Sendai, Japan),

and were cultured based on the protocol of the previous study [11].

2.3. Cell proliferation assays

The status of cell proliferation of EMTOKA cells was measured using WST-8 [2-(2-methoxy-4-nitro-phenyl)-3-(4-nitrophenyl)-5-(2,4-disulfophenyl)-2H-tetrazolium, monosodium salt] method (Cell Counting Kit-8 (Dojindo Inc., Kumamoto, Japan)) [12]. Ten microliters of 5 mM WST-8 was added to 100 μl of cells, which were then incubated for 1 h at 37 °C in 5% CO_2–95% air atmosphere. Optical densities (OD, 450 nm) were obtained with a SpectraMax 190 microplate reader (Molecular Devices, Corp., CA, USA) and Softmax Pro 4.3 microplate analysis software (Molecular Devices, Corp.). The status of proliferation (%) was calculated according to the following equation: (cell OD value after test materials treated/vehicle control cell OD value) ×100. EMTOKA cells were also measured using the trypan blue exclusion (TBE) test. Trypan blue-positive cells were determined as dead cells using a hemocytometer under light microscopy. The ratio of cell proliferation (%) was calculated according to the following equation: (1 viable cell number after test materials treated/vehicle control cell number) ×100.

2.4. Microarray analysis

We employed BD Atlas Custom Nylon Membrane Hybridization and Analysis (Clontech company, CA, USA) for microarray analysis. The Atlas human cancer 1.2 array (Cancer array) was used in this study. Cancer array was a nylon membrane, which contained 1176 cDNA fragments of known human oncogenes including control housekeeping genes. We compared the differences of the patterns of gene expressions induced by 10 pM E2, 10 pM DES, and 1 μM DES. The quality of RNA extracted from EMTOKA cells was confirmed by the presence of 28S and 18S ribosomal bands, respectively. Twenty micrograms of each total RNA was reverse-transcribed in the presence of [α-^{32}P] dATP using the Atlus Pure Total RNA Labeling System (K1038-1, Clontech company). Hybridization of the ^{32}P labeled cDNA with the array membranes was performed using ExpressHyb Solution (Clontech company). The membrane was exposed to Atlas

Image 2.01 Software V1213-1 (Clontech company), and the hybridization signals were generated as phosphorimages and subsequently was subjected to thorough analysis using Atlas Image 2.01 Software V1213-1 (Clontech company) in accordance to the manufacturer's instructions. The term in this case, normalization, refers to using the expression levels of one or more housekeeping genes as standard for measuring the expression levels of other genes. Housekeeping genes were present in all the cells examined. Data from each array was subjected to hierarchical clustering analysis and visualization using the software copyright Stanford University 1998–1999 (http://rana.stanford.edu) to generate tree structures based on the degree of similarity, as well as matrices comparing the levels of expression of individual genes in each samples [13].

2.5. Real-time PCR

Real-time PCR was carried out using the Light Cycler System (Roche Diagnostics GmbH, Mannheim, Germany) using the SYBR Green PCR kit (Roche Diagnostics GmbH). PCR was set up at 4 mM $MgCl_2$, 10 pmol/l of each primer (Table 1) [14–16] and 2.5 U *Taq* DNA polymerase (InVitrogen Life Technologies, Inc.). An initial denaturing step of 95 °C for 1 min was followed by 40 cycles, respectively, of 95 °C for 0 s (no holding time); 15 s annealing at 62 °C (*c-myc*) or 60 °C (ERα, β, and glyceraldehyde-3-phosphate dehydrogenase (GAPDH)); and extension for 15 s at 72 °C. Following PCR, these products were resolved on 2% agarose ethidium bromide gel to verify that only a single band was present in the amplification reaction. PCR for *pS2* mRNA in MCF-7 treated with E2 and/or ICI was performed according to the previous study [17]. All gel images were captured with Image Reader LAS-1000 Pro. (Fuji Photo Film Co., Ltd, Tokyo, Japan) under UV transillumination. In initial experiments, PCR products were purified and subjected to direct sequencing (ABI PRISM BigDye Terminator v3.0 Cycle sequencing Kit and ABI PRISM 310 Genetic Analyzer, Applied Biosystems, CA, USA) to verify amplification of the correct sequences. Negative control experiments included those lacking cDNA substrates to confirm the presence of exogenous contaminant DNA. No amplified products

Table 1
Primer sequences used in RT-PCR analysis

cDNA	GB#		Sequence	cDNA position	Size (bp)	References
ERα	M12674	Forward Reverse	5'-AAG AGC TGC CAG GCC TGC-3' 5'-TTG GCA GCT CTC ATG TCT CC-3'	702–869	168	Ishizuka et al. [14]
ERβ	AB006590	Forward Reverse	5'-GCT CAA TTC CAG TAT GTA CC-3' 5'-GGA CCA CAT TTT TGC ACT-3'	1313–1537	225	Ishizuka et al. [14]
c-myc	K02276	Forward Reverse	5'-ACC ACC GCA GCG ACT CTG A-3' 5'-TCC AGC AGA AGG TGA TCC AGA CT-3'	1297–1413	117	Latil et al. [15]
GAPDH	M33197	Forward Reverse	5'-TGA ACG GGA GCT CAC TGG-3' 5'-TCC ACC ACC CTG TTG CTG TA-3'	731–1037	307	Miki et al. [16]

GB#, GeneBank accession number.

were detected under these conditions. The quantification data were analyzed by the Light Cycler software version 3.3.5 (Roch Diagnostics GmbH). To determine the quantity of c-*myc* mRNA transcripts, cDNAs of known concentration for c-*myc* and the housekeeping gene, GAPDH were used to generate standard curves for real-time qPCR. The mRNA levels in each case were represented as a ratio of GAPDH, and evaluated as a ratio (%) compared with that of each control. Conventional quantitative PCR (qPCR) requires the utilization of a defined cDNA in the construction of a standard curve, but employment of the Light Cycler utilizing a purified PCR product cDNA of known concentration can semi-quantify PCR products [16].

2.6. Antibodies

Monoclonal antibodies used for immunocytochemistry (ICC) and/or immunoblotting (IB) are summarized as follows. Antibodies for the two isoforms of ER, ERα (NCL-ER-6F11) and ERβ (ER-β−14C8) were purchased from Novocastra Laboratories Ltd (Newcastle, UK) and GeneTex, Inc. (Texas, USA), respectively. Antibody for c-MYC (1-6E10) was purchased from Cambridge Research Biochemicals, Inc. (Cambridge, UK). Progesterone receptor (MAB429) and Ki-67 (MIB-1) were purchased from CHEMICON International Inc. (CA, USA), and DAKO Cytomation Co., Ltd (Glostrup, Denmark), respectively. The dilutions of primary antibodies for ICC/IB were as follows: ERα, 1:50/1:100; ERβ, 1:1500/1:3000; c-*myc* oncogene 1:600/1:2000; PR, 1:50/–; Ki-67, 1:100/– [18–20].

Antigen retrievals for ICC were as follows: ERα and β, microwave; c-MYC, non-treatment; PR and Ki-67, autoclave.

2.7. Immunocytochemistry

Cells were grown directly on clean and sterilized silan-coated glass slides (Matsunami Galass Ind., Ltd, Tokyo, Japan) under culture conditions described above. Glass slides were washed thoroughly in PBS and then fixed with 10% formaldehyde for 30 min. Cells were immunostained by a biotin–streptavidin method using Histofine kit (Nichirei Co. Ltd, Tokyo, Japan) and have been previously described in detail [20]. These reacted sections were incubated with normal goat serum for 30 min. These slides were further incubated with primary antibodies for 12–18 h in a moist chamber at 4 °C. The antigen–antibody complex was then visualized with 3,3'-diaminobenzidine (DAB) solution (1 mM DAB, 50 mM Tris–HCl buffer, pH 7.6, and 0.006% H_2O_2), and counterstained with hematoxylin. Normal IgG was used instead of the primary antibody as a negative control. No specific immunoreactivity was detected in these tissue sections.

2.8. Immunoblotting

The cell protein was extracted in 500 μl of cold triple detergent buffer [21]. A protein Assay Rapid Kit (Wako Pure Chemicals Industries, Ltd) was used to determine the concentration of protein by the pyrogallol red-molybdate method. OD (600 nm) of

protein was obtained with a SpectraMax 190 microplate reader (Molecular Devices, Corp.) and Softmax Pro 4.3 microplate analysis software (Molecular Devices, Corp.).

IB was performed using 20 μg of protein. After optimizing the conditions of experiments, 20 μg of protein specimens were denatured at 95 °C in 2% SDS, 10% glycerol, 62.5 mM Tris (pH 6.8), and 5% 2-mercaptoethanol and electrophoresed at 150 V through a 3.9% stacking gel and 12.5% resolving SDS-polyacrylamide gel (InVitrogen Life Technologies, Inc.). Following electrophoresis, proteins were transferred onto Hybond P polyvinylidene difluoride membrane (Amersham Biosciences Corp., NJ, USA) using Mini Trans-Blot Cell and Power/Pac 200 (Bio-Rad Laboratories Inc., CA, USA). Non-specific binding sites were blocked by immersing the membrane in 5% skim milk (Becton Dickinson and Company, NJ, USA), for 1 h at room temperature, washed twice in 0.05% Tween 20 and PBS (PBS–T), respectively, and incubated with human c-myc antiserum (Cambridge Research Camicals, Inc.) in PBS–T for 18 h at 4 °C. After washing in PBS–T, reacted membranes were incubated with a 1:1000 dilution of anti-mouse IgG horseradish peroxidase (Amersham Biosciences Corp.) conjugated for 1 h at room temperature. Protein bands were subsequently detected using the ECL Plus Western blotting detection reagent (Amersham Biosciences Corp.) and visualized with Las-1000 cooled CCD-camera chemiluminescent image analyzer (Fuji Photo Film Co., Ltd). The relative abundance of reacted signals for c-myc was subsequently quantified as OD value with Science Lab 99 Image Gauge 3.2 software (Fuji Photo Film Co., Ltd). The intensity for c-MYC immunoreactivity (OD value) was evaluated as a ratio (%) compared with that of control cells.

2.9. Statistical analysis

Results were expressed as mean ± SD. Statistical analysis was performed with the StatView 5.0 J software (SAS Institute Inc., NC, USA). All data were analyzed by analysis of variance (ANOVA) followed by post hoc Bonferroni/Dunnet multiple comparison test. A P-value < 0.05 was considered to indicate statistical significance.

3. Results

3.1. Characteristics of EMTOKA cell line

EMTOKA cells used in this study expressed protein and mRNA transcript of ERβ. The levels of their expressions were relatively high in ICC, RT-PCR, and IB (Fig. 1A–C, respectively). Immunoreactivity (ICC, Fig. 1A; IB, data not shown) of ERα and its regulated gene, PR were not detected in EMTOKA cells. ERα (Fig. 1B) and PR (data not shown) mRNA transcripts were also not at detectable levels in EMTOKA cells using RT-PCR. In intact cells, marked immunoreactivity of c-myc was detected in ICC (Fig. 1A), but its level was low in IB (Fig. 5). c-myc mRNA transcript was also detected using RT-PCR (Fig. 5). Cell proliferation marker, Ki-67 (MIB-1) was detected in intact EMTOKA cells using ICC (Fig. 1).

3.2. Cell proliferation

The results of the cell proliferation assays using WST-8 are summarized in Figs. 2 and 3. In DES treated cells, no significant changes of the cell number were detected with low to middle doses of DES (10^{-12}–10^{-7} M). There was a significant increase in the number of the cells after DES treatment of 72 h with high-dose, 10^{-7} and 10^{-6} M. Morphological features suggestive of toxicity including apoptosis-like changes were detected only at highest concentration (10^{-5} M) of DES treatment. E2 treatment of 10^{-11} M significantly increased the cell number. Middle to high-doses of E2 was not associated with significant increment of the cell number. Results of TBE test were consistent with those of WST-8 cell proliferation assay (data not shown). Exposure of EMTOKA cells to serially diluted DES (expect for 10^{-5} M) or E2 were not associated with morphological changes, but highest dose of DES (10^{-5} M) was associated with apoptosis like nucleic changes (data not shown). The solvent ethanol (maximal dose, 0.1%) had no effects on cell proliferation and morphology of EMTOKA cells. In both TBE test and WST-8 assay (Fig. 3 demonstrated results of WST-8 assay), the cell number of EMTOKA cells treated by 100 nM or 1 μM DES for 48 h (100 nM) and 72 h (100 nM and 1 μM) was
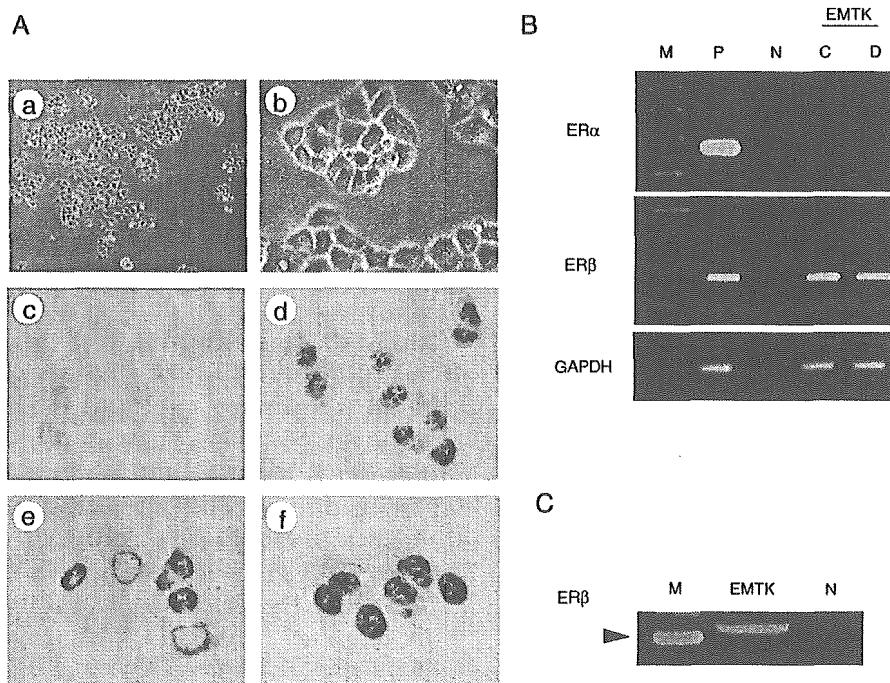
Fig. 1. Characteristics of EMTOKA cell line. (A) Phase contrast microscopic analysis of EMTOKA cells morphology (a and b). EMTOKA cells are cobble-stone shaped. Immunoreactivity of ERα was not detectable in EMTOKA cell (c). Immunoreactivity of ERβ was markedly detected in nuclei of the cells (d). c-myc and Ki-67 immunoreactivities were also detected in nuclei of the cells (e, c-myc; f, Ki-67). Original magnification: ×100 (a) and ×400 (b–f). (B) RT-PCR for ERα and β in EMTOKA cells. ERα mRNA transcript was detected in T-47D breast carcinoma cells as positive control (P), but not detected in EMTOKA cells (EMTK). ERβ mRNA transcript was detected in both T-47D and EMTOKA cells. (M, molecular marker; N, lack of cDNA as negative control; C, intact EMTOKA cells as control; D, DES treatment cells.) (C) Immunoblotting for ERβ in EMTOKA cells. ERβ protein was detected in EMTOKA (EMTK) cells. (M, molecular marker; arrowhead, 60 kDa).

significantly higher than that treated for 24 h. Low-dose of DES (10 pM) exerted no effects on the status of cell proliferation treated for 24–72 h, but low-dose of E2 resulted in significant increment of the cell number at both 24 and 48 h.

3.3. Microarray analysis in EMTOKA cells

In clustering analysis of the expression levels of each gene, the expression profiles treated with 1 μM DES were clearly discernible from those treated with either 10 pM DES or 10 pM E2 treatments. We then analyzed the clustering patterns of expression patterns of 1 μM DES, 10 pM DES, and 10 pM E2. Cluster analysis grouped 1700 differentially regulated genes into six well-defined expression profiles or groups (groups A–F), which are summarized in Fig. 4. Groups A and D represent all down- or up-regulated genes in all treatment, respectively. Groups B and E

represented up- or down-regulated genes only in 1 μM DES treated cells. Groups C and F represented down-regulated genes only in 10 pM E2, or up-regulated genes only in 10 pM E2, respectively.

In this study, we focused on group B, up-regulated genes associated with only high-dose of DES treatment in order to study possible teratogenic or toxic effects of DES on human primitive Müllerian cells. Group B consists of 48 genes, which were up-regulated twice or more than control (Table 2). c-myc (GeneBank accession number (GB): V00568) and its target genes (Myc cancer Gene (http://www.myccancergene.org/index.asp, Johns Hopkins University School of Medicine and Johns Hopkins Health System, 2004)) (Table 3) [22–25] were included in these genes of group B. E2 and DES were reported to regulate c-myc oncogene [26]. Therefore, we further examined whether c-myc was increased by E2 or DES treatment using qRT-PCR and IB in EMTOKA cells.
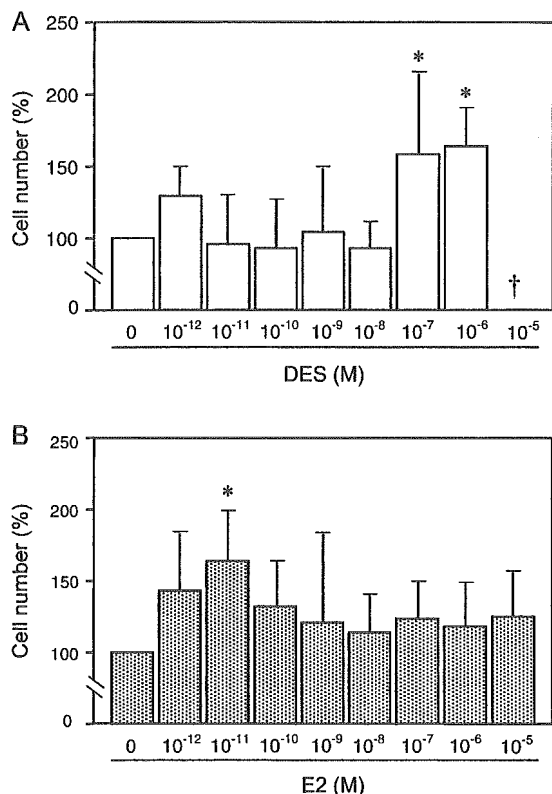
Fig. 2. Dose-dependent proliferation of EMTOKA cells. (DES (A) and E2 (B)). There was a significant increase in the number of cells after treated for 72 h with high-dose, 10^{-7} and 10^{-6} M DES in WST-8 assay. Significant decrement of the cell number was noted at highest concentration (10^{-5} M) of DES in WST-8 assay, but the morphological features of these cells were apoptotic cell death in trypan blue assay (†). In E2 treatment, low-dose of E2, 10^{-11} M significantly increased the cell number. Middle to high-doses of E2 had no significantly effects on the number of cells. Results of TBE test were consistent with those of WST-8 cell proliferation assay (data not shown). The numbers of EMTOKA cells treated by DES or E2 were evaluated as a ratio (%) compared with that of the number treated with vehicle only. Treatment of only vehicle was denoted 0 M. *, $P < 0.05$ vs. vehicle (0.05% ethanol) control.

3.4. Expression levels of c-myc in EMTOKA cells

Both c-*myc* protein and mRNA transcript were primarily expressed in EMTOKA cell (Figs. 1 and 5). In 1 µM DES treatment, significantly high levels of c-*myc* protein were detected, but E2 did not increase the levels of c-*myc* protein expression (Fig. 5A, B). As for protein analysis, c-*myc* mRNA transcripts were
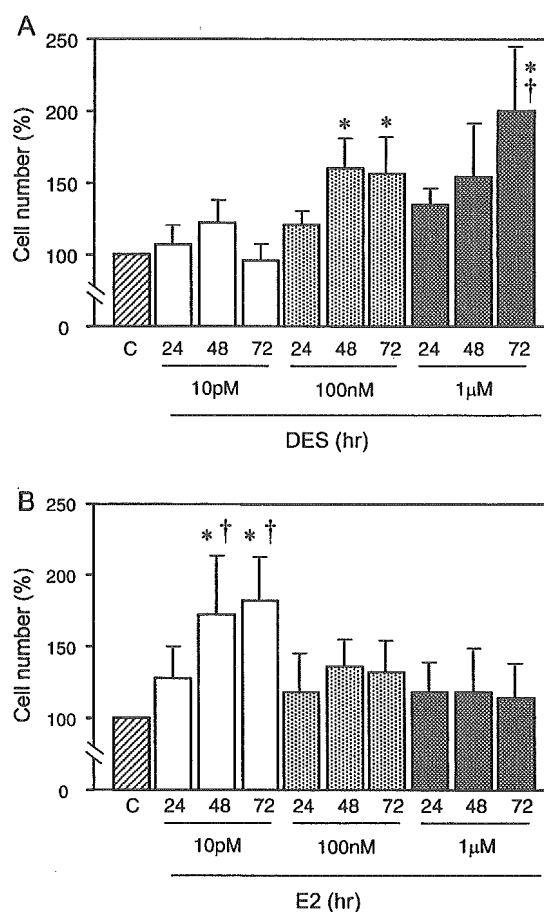

Fig. 3. Time-dependent proliferation of EMTOKA cells. (DES (A) and E2 (B)). The number of the cells treated by 100 nM or 1 µM DES for 48 h (100 nM) and 72 h (100 nM and 1 µM) were significantly higher than treated for 24 h. Low-dose of DES (10 pM) exerted no effects on cell proliferation treated for 24–72 h. The numbers of the cells treated with low-dose of E2 were significantly higher at 24 and 48 h. Results of TBE test were consistent with those of WST-8 cell proliferation assay (data not shown). The cell number of EMTOKA cells treated with DES or E2 were evaluated as a ratio (%) compared with that of the cell number treated with vehicle only. *, $P < 0.05$ vs. vehicle (0.05% ethanol) control (C); †, $P < 0.05$ vs. treatment for 24 h in same concentration.

In addition, DES and E2 regulated gene, c-*fos*, c-*jun*, homeobox genes expressions were demonstrated in Table 4. c-*jun* was found to be down regulated by LD-DES treatment, but HD-DES treatment up-regulated c-*jun* expression. c-*fos* was up-regulated only by HD-DES treatment, but its level was very low. Homeobox genes, HOXA4 (GB: M26679) and HOXB5 (GB: M92299) genes were decreased by HD-DES treatment.
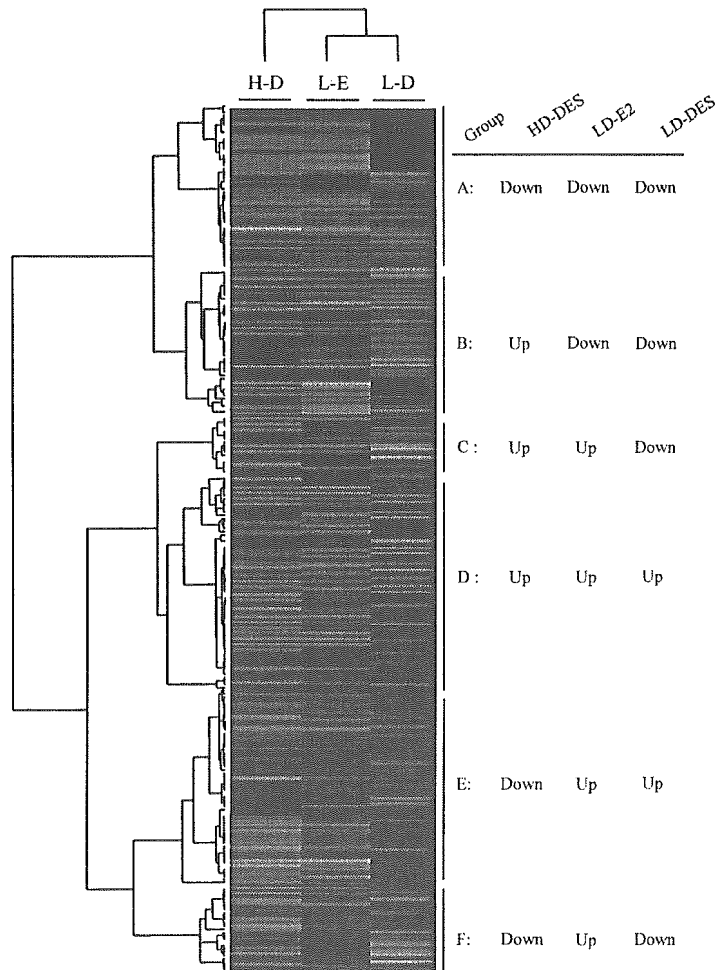
Fig. 4. In clustering analysis of the expression levels of each gene in EMTOKA cells treated with low-dose E2 and low-/high-dose DES. The expression profiles of 1 µM DES would be clearly distinguished from their expression of 10 pM DES and 10 pM E2. Groups A and D represented down- or up-regulated genes in all treatment, respectively. Groups B and E represented up- or down-regulated genes only in 1 µM DES treated cells. Groups C and F represented down-regulated genes only in 10 pM E2, or up-regulated genes only in 10 pM E2, respectively. All the genes were classified into two patterns: up, up-regulated genes; down, down-regulated genes by low- and/or high-dose E2 and DES treatment. H-D, high-dose (HD) DES; L-E, low-dose (LD) E2; L-D, low-dose (LD) DES.

significantly higher in DES, but not E2 treated cells (Fig. 5C). Furthermore, the estrogen receptor antagonist ICI failed to diminish the effects of DES on induction of c-myc mRNA transcript in EMTOKA cell (Fig. 5C). We confirmed that 1 µM ICI decreased pS2 mRNA transcript induced by E2 (10^{-8} M) treatments (Fig. 5D). Therefore, examination of inhibitory effects of ICI was considered to be performed with reasonable accuracy.

4. Discussion

In this study, we used EMTOKA cell line, which was established from a human uterine carcinoma obtained from a patient [9]. EMTOKA 5E4 clone also established by Gorai et al. [10] was one of the few cell lines associated with features of a human primitive Müllerian duct cell. Estrogen plays important roles in

Table 2
Genes induced by high-dose DES treatment in EMTOKA cells

No.	GB#	Gene	Symbol	Ratio
1	M77234	40S ribosomal protein S3A	RPS3A	3.8
2	J03075	Protein kinase C substrate 80-kDa protein heavy chain	PKCSH	3.6
3	X04106	Calpain	CAPNS1	3.4
4	X17620	Non-metastatic cells 1, protein (NM23A) expressed in	NME1	3.2
5	L16785	Non-metastatic cells 2, protein (NM23B) expressed in	NME2	3.1
6	M35410	Insulin-like growth factor binding protein 2, 36 kDa	IGFBP2	3.0
7	L05500	Adenylate cyclase 1 (brain)	ADCY1	3.0
8	D38305	Transducer of ERBB2, 1	TOB1	2.8
9	S40706	DNA-damage-inducible transcript 3	DDIT3	2.8
10	M12529	Apolipoprotein E	APOE	2.8
11	X15218	v-Ski sarcoma viral oncogene homolog	SKI	2.6
12	AF040105	Chromosome 6 open reading frame 108	C6orf108	2.6
13	M74816	Clusterin	CLU	2.6
14	M16038	v-yes-1 Yamaguchi sarcoma viral related oncogene homolog	LYN	2.5
15	L07493	Replication protein A3, 14 kDa	RPA3	2.5
16	X55504	HOM-TES-103 tumor antigen-like	HOM-TES-103	2.5
17	L37882	Frizzled homolog 2	FZD2	2.5
18	X06745	Polymerase (DNA directed), alpha	POLA	2.5
19	M26708	Prothymosin, alpha (gene sequence 28)	PTMA	2.4
20	X54942	CDC28 protein kinase regulatory subunit 2	CKS2	2.4
21	L33264	Cyclin-dependent kinase (CDC2-like) 10	CDK10	2.4
22	U21092	TNF receptor-associated factor 3	TRAF3	2.4
23	AF035606	Programmed cell death 6	PDCD6	2.4
24	U05340	CDC20 cell division cycle 20 homolog (S. cerevisiae)	CDC20	2.3
25	X57766	Matrix metalloproteinase 11 (stromelysin 3)	MMP11	2.3
26	X66364	Cyclin-dependent kinase 5	CDK5	2.3
27	X57346	Tyrosine 3-monooxygenase/tryptophan 5-monooxygenase activation protein	YWHAB	2.3
28	U07418	MutL homolog 1, colon cancer, nonpolyposis type 2 (E. coli)	MLH1	2.2
29	U51004	Histidine triad nucleotide binding protein 1	HINT	2.2
30	L05624	Mitogen-activated protein kinase kinase 1	MAP2K1	2.2
31	V00568	v-Myc myelocytomatosis viral oncogene homolog (avian)	MYC	2.2
32	M19722	Gardner–Rasheed feline sarcoma viral (v-fgr) oncogene homolog	FGR	2.2
33	L13738	Activated Cdc42-associated kinase 1	ACK1	2.1
34	L07540	Replication factor C (activator 1) 5, 36.5 kDa	RFC5	2.1
35	M64788	RAP1, GTPase activating protein 1	RAP1GA1	2.1
36	M62880	Integrin, beta 7	ITGB7	2.1
37	D15057	Defender against cell death 1	DAD1	2.1
38	S56143	Adenosine A1 receptor	ADORA1	2.1
39	M81757	Ribosomal protein S19	RPS19	2.1
40	X76132	Deleted in colorectal carcinoma	DCC	2.0
41	U04806	Fms-related tyrosine kinase 3 ligand	FLT3LG	2.0
42	M97935	Signal transducer and activator of transcription 1, 91 kDa	STAT1	2.0
43	X69550	Rho GDP dissociation inhibitor (GDI) alpha	ARHGDI	2.0
44	U09607	Janus kinase 3 (a protein tyrosine kinase, leukocyte)	JAK3	2.0
45	X16707	FOS-like antigen 1	FOSL1	2.0
46	X74979	Discoidin domain receptor family, member 1	DDR1	2.0
47	X54941	CDC28 protein kinase regulatory subunit 1B	CKS1B	2.0
48	U22398	Cyclin-dependent kinase inhibitor 1C (p57, Kip2)	CDKN1C	2.0

GB#, GeneBank accession number; Ratio, compared with control gene expressions.

Table 3
c-myc target genes induced by high-dose DES treatment in EMTOKA cells

GB#	Symbol	Function	Regulation	ER	Organism	Reference
J03075	PKCSH	Signal transduction	–	–	H	www.[a]
X04106	CAPNS1	Apoptosis	up	–	H	Xynos et al. [24]
X17620	NME1	Transcription Factor	up	–	H, R, C	www.[a]
L16785	NME2	Metabolism	up	–	R	www.[a]
AF040105	C6orf108	Cell growth	up	–	H, R	Lewis et al. [22]
M26708	PTMA	DNA repair	up	P	H, M, R	www.[a]
X54942	CKS2	Cell cycle	up	P	H, R	www.[a]
U07418	MLH1	DNA repair	*	–	Y	Partlin et al. [25]
U51004	HINT	Signal transduction	–	–	H	www.[a]
D15057	DAD1	Anti-apoptosis	up	–	H	Xynos et al. [24]
M81757	RPS19	Protein synthesis	up	–	H, R	www.[a]
M97935	STAT1	Transcription factor	up	–	H, M	Ramana et al. [23]
X16707	FOSL1	Transcription factor	up	–	H	www.[a]

All the data, c-myc target genes in Table 3 were picked up from Table 2. GB#, GeneBank accession number; –, unknown; *, interaction with c-myc; P, chimeric myc-estrogen receptor system was employed; H, human; R, rat; M, mouse; C, chicken; Y, yeast.

[a] www., Myc Cancer Gene (http://www.myccancergene.org/index.asp).

female reproductive system including uterus, cervix, and vaginal development [27,28], but there have been no reports regarding the roles of estrogen including ERs expression in EMTOKA cells. ERβ was expressed in EMTOKA cells and the cell proliferation in response to both E2 and DES, but ER inhibitor, ICI, could not reverse or prevent these reactions. HD-DES could stimulate cell proliferation of EMTOKA cells, but LD-DES and HD-E2 could not necessarily increase the cell numbers. In human breast cancer, MCF-7 cell proliferation assay (E-screen assay) [29], DES exhibited a broad peak ranging from 10^{-9} to 10^{-6} M (low-dose to high-dose), and E2 exhibited a peak in 3×10^{-11} M. The status of cell proliferation was also evaluated at the treatment of the same concentrations described above for both E2 and DES except for LD-DES in EMTOKA cells. These E2 and DES induced cell proliferations could not be reversed or prevented by ICI, which also indicated that this cell proliferation may not be exerted through ERs or may be though ER independent pathway. In vivo study using fetal female rat, DES increased Müllerian duct cell proliferation in the proximal epithelium and mesenchyme, but decreased cell proliferation in caudal epithelium, and DES was postulated to exert these effects through both ERβ1 and ERβ2 [30]. Altered expression of ERα, but not of ERβ was also reported in adult male and female reproductive tracts after neonatal DES exposure in reproductive tracts of

ERα and/or β knockout mouse, although developments were normal during the prenatal and neonatal stages [30]. Couse et al. [31] further reported that the absence of DES-induced abnormalities in reproductive tract of ERα knockout mouse was consistent with a predominant role of ERα in mediating the detrimental effects of DES in female reproductive tract development. Expression of ERα and β in normal human embryo and/or fetal tissues were largely unknown, but Takeyama et al. [32] reported that ERβ was predominantly expressed in the genital tract of human fetal female tissues. In the human embryo/fetus, ERβ is considered to play some roles in the maintenance of development, but HD-DES may stimulate EMTOKA cell proliferation through ERβ independent pathway. It awaits further investigations for clarification.

Estrogen induced cell proliferation in quiescent cells is generally associated with increased expression of immediate early estrogen response genes such as proto-oncogenes such as c-jun, c-fos, and c-myc [26]. Zheng and Hendry [26] demonstrated that immunoreactivities of c-jun, c-fos, and c-myc were all increased in DES-treated ovariectomised hamster uterus. In our microarray analysis, both c-jun and c-fos were not up regulated by both E2 and LD-DES treatments. However, in HD-DES-treated EMTOKA cells, expression of c-myc and its response genes was markedly increased, while low levels of c-jun and
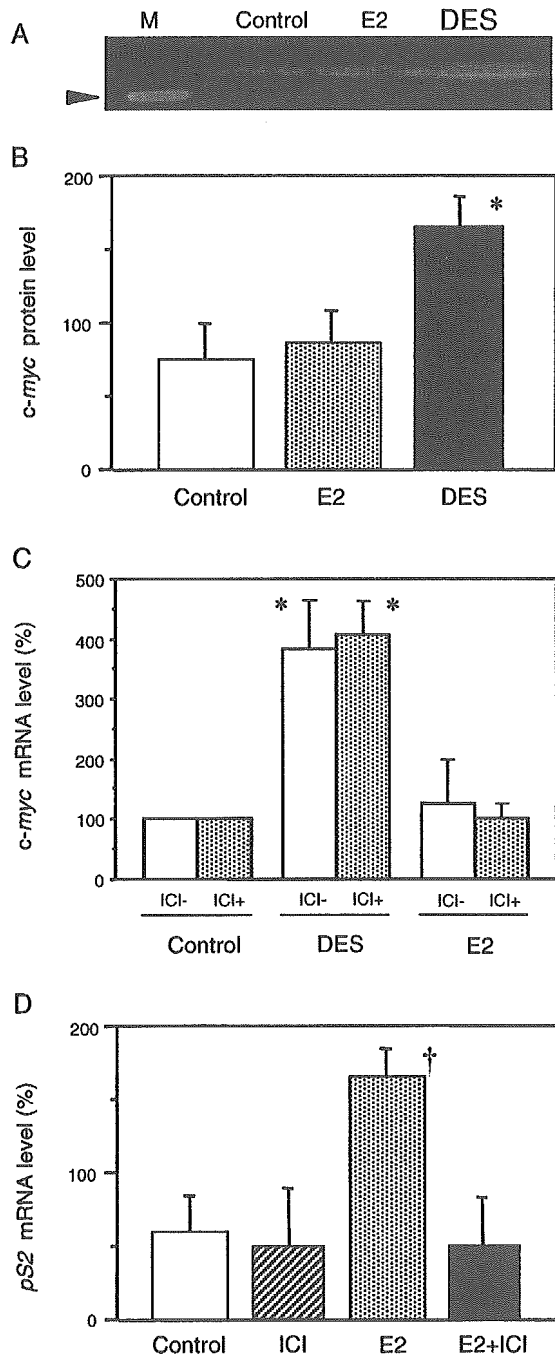
c-*fos* expressions were detected in these systems. c-*myc* has ER response element, and has been demonstrated to be induced by E2 and DES treatment via ER [26] (Table 4). In this study, c-*myc* mRNA transcript and protein were demonstrated to be increased by HD-DES, but not by LD-E2 and LD-DES. Furthermore, ICI compound failed to decrease the effects of HD-DES on induction of both c-*myc* mRNA transcript and protein. DES was strongly correlated with the abnormalities and/or carcinogenesis in embryo to fetal reproductive development by induction of c-*myc* oncogene through ER independent pathway. Overexpression of the c-*myc* gene in cervical squamous cell carcinoma has been demonstrated to be associated with significant increment of early disease relapse following surgery [33]. c-*myc* is therefore postulated to play important roles in carcinogenesis induced by DES in human reproductive system. Expression of the c-*myc* gene is in general closely related to the G1-S transition by activating cyclin–cyclin dependent kinases (CDK) complexes [34]. Results of our present study also demonstrated up-regulation of CDKs including CDK 10 and 5 consistent with those report above. c-*myc* interacts with the MutL homologue MLH1 that is related to DNA repair [25]. Furthermore, markedly up-regulated genes also included *rcl* in our study, a c-*myc* responsive growth related gene, cell cycle regulators such as G1/S specific cyclin D1, and apoptosis regulators including calpain and defender against cell death (DAD1) [24]. The expression of c-*myc* is regulated by the c-*myc* transcriptional factor PuF [24]. These findings all suggest that various genes up- or down regulated by c-*myc* may lead to cell turnover and differentiation in human primitive genital tract. At one level, both c-*myc* and N-*myc* are considered essential for vertebrate development [35]. In normal

Fig. 5. c-*myc* protein and mRNA expressions in 1 μM DES or 10 pM E2 exposed EMTOKA cells for 48 h. (A) Weak immunoreactivity of c-*myc* was detected in the vehicle (0.05% ethanol) control and E2 exposed cells. Marked immunoreactivity of c-*myc* was detected in DES exposed cells (arrow head, 60 kDa). (B) c-*myc* protein expression was low in the intact and E2 exposed cells,

whereas the significantly high levels of c-*myc* protein were detected in DES exposed cells. c-*myc* protein level was demonstrated as relative OD (arbitrary unit). (C) The effects of estrogen receptor antagonist ICI on c-*myc* transcripts in DES or E2 treated EMTOKA cells. DES and E2 were treated with (ICI+) or without (ICI−) ICI. There were no changes of ICI pre-treatment in both vehicle (0.05% ethanol) control (Control) and E2. ICI could not diminish the effects of DES on induction of c-*myc* mRNA transcript. (D) ICI decreased c-*myc* mRNA transcript in MCF-7 induced by E2 (10 pM) treatments. *, $P < 0.05$ vs. vehicle (0.05% ethanol) control (Control) or E2. †, $P < 0.05$ vs. Control, ICI, and E2 + ICI.

Table 4
Genes induced by E2 and DES treatment in EMTOKA cells

No.	GB #	Gene	Symbol	Ratio		
				L-E	L-D	H-D
1	V00568	v-Myc myelocytomatosis viral oncogene homolog (avian)	MYC	−1.4	−	2.2
2	J04111	v-Jun sarcoma virus 17 oncogene homolog (avian)	JUN	−	−1.4	1.4
3	K00650	v-Fos FBJ murine osteosarcoma viral oncogene homolog	FOS	−	−	1.5
4	M26679	Homeo box A5	HOXA5	−	−	−2.7
5	M92299	Homeo box B5	HOXB5	−	−	−1.5

GB#, GeneBank accession number; L-E, low-dose (10 pM) estradiol; L-D, low-dose (10 pM) diethylstilbestrol; H-D, high-dose (10 μM) diethylstilbestrol; Ratio, compared with control gene expressions.

Müllerian duct cells, the expression of c-myc result in inhibition of programmed cell death in normal development and/or apoptosis in the cells associated with DNA damages. In addition, accumulation of these effects may result in permanental genomic imprinting. Uncontrolled expression of imprinting genes can be associated with hereditary and sporadic cancer development [36]. These findings all suggest that disorganized imprinting may affect embryogenesis and may result in several disease symptoms including DES-adenosis. In addition to DES-daughter, mother treated with DES result in increased risks for breast cancer [37]. Li et al. [38] demonstrated that neonatal, but not mature mice treated with DES were associated with demethylation of estrogen-responsive gene (lactoferrin), which is consistent with permanental genomic imprinting. However, it is also true that c-myc is associated with a wide variety of functions [34], and it awaits further investigations for clarifying about DES induced inherited abnormality and/or directly carcinogenesis of reproductive system.

The importance of homeobox (HOX) genes in the regulation of mammalian development has been well established, and differential expression of HOX genes occurs in several cancers [39]. In human uterine or cervical cells, HOX genes including HOXA9 and HOXB5 genes were expressed in normal cervical tissues [40]. In addition, DES induced HOXA9 and HOXA10 genes expression to levels approximately 2-fold compared to estradiol [41]. In our present study, DES and E2 treatment did not affect levels of HOXA9 and HOXA10 genes expression, but did down regulate HOXA5 and HOXB5 genes. HOXA5 gene has been demonstrated to activate transcription

of the key tumor suppressor gene p53, and down regulation of HOXA5 gene leads may result in loss of p53 gene expression [42]. Reduction of HOXA5 as a result of HD-DES treatment may be also subsequently result in decreased p53. Further investigations were required for clarifications.

References

[1] K. Kruse, D. Lauver, K. Hanson, Clinical implications of DES, Nurse Pract. 28 (2003) 26–35.

[2] W.J. Dieckmann, M.E. Davis, L.M. Rynkiewicz, R.E. Pottinger, Does the administration of diethylstilbestrol during pregnancy have therapeutic value? Am. J. Obstet. Gynecol. 66 (1953) 1062–1081.

[3] A.L. Herbst, H. Ulfelder, D.C. Poskanzer, Adenocarcinoma of the vagina. Association of maternal stilbestrol therapy with tumor appearance in young women, N. Engl. J. Med. 284 (1971) 878–881.

[4] S.J. Robboy, R. Virata, W.M. Szyfelbein, P.A. Hatab, J.R. Goeliner, S.P. Mcgorray, et al., Dysplasia and cytologic findings in 4589 young women enrolled in diethylstilbestrol-adenosis (DESAD) project, Am. J. Obstet. Gynecol. 140 (1981) 579–586.

[5] G.E. Barness, S. Gunasekaran, R. Scully, Reproductive system in: G.E. Barness (Ed.), *Potter's* Pathology of the Fetus and Infant fourth ed., Mosby/Year Book, St Louis, 1997, pp. 1202–1241. (Chapter 27).

[6] J.G. Forsberg, Animal model of human disease: adenosis and clear-cell carcinomas of vagina and cervix, Am. J. Pathol. 84 (1976) 669–672.

[7] T. Kitamura, S. Nishimura, K. Sasahara, M. Yoshida, J. Ando, M. Takahashi, et al., Transplacental administration of diethylstilbestrol (DES) caused lesions in female reproductive organs of Donryu rats, including endometrial neoplasia, Cancer Lett. 141 (1999) 219–228.

[8] F.J. Leary, L.J. Ressegui, L.T. Kurland, P.C. O'Brien, R.F. Emslander, K.L. Noller, Males exposed in utero to diethylstilbestrol, J. Am. Med. Assoc. 252 (1984) 2984–2989.

[9] I. Gorai, C. Doi, H. Minaguch, Establishment and characterization of carcinosarcoma cell line of the human uterus, Cancer 71 (1993) 775–786.

[10] I. Gorai, T. Yanagibashi, A. Taki, K. Udagawa, E. Miyagi, T. Nakazawa, et al., Uterine carcinosarcoma is derived from a single stem cell: an in vitro study, Int. J. Cancer 72 (1997) 821–827.

[11] M. Venditti, B. Iwasiow, F.W. Orr, R.P.C. Shiu, C-*myc* gene expression alone is sufficient to confer resistance to antiestrogen in human breast cancer cells, Int. J. Cancer 99 (2002) 35–42.

[12] I. Isobe, M. Michikawa, K. Yanagisawa, Enhancement of MTT, a tetrazolium salt, exocytosis by amyroid beta-protein and chloroquine in cultured rat astrocytes, Neurosci. Lett. 266 (1999) 129–132.

[13] M.B. Eisen, P.T. Spellman, P.O. Brown, D. Bostein, Cluster analysis and display of genome-wide expression patterns, Proc. Natl Acad. Sci. 95 (1998) 14863–14868.

[14] M. Ishizuka, M. Hatori, T. Suzuki, Y. Miki, A.D. Darnel, C. Tazawa, et al., Sex steroid receptors in rheumatoid arthritis, Clin. Sci. (Lond.) 106 (2004) 293–300.

[15] A. Latil, D. Vidaud, A. Valeri, G. Fournier, M. Viaud, R. Lidereau, et al., *htert* expression correlates with *MYC* over-expression in human prostate cancer, Int. J. Cancer 89 (2000) 172–176.

[16] Y. Miki, T. Nakata, T. Suzuki, A.D. Darnel, T. Moriya, C. Kaneko, et al., Systemic distribution of steroid sulfatase and estrogen sulfotransferase in human adult and fetal tissues, J. Clin. Endocrinol. Metab. 87 (2002) 5760–5768.

[17] M. Colombel, R. Dante, R. Bouvier, S. Ribieras, C. Pangaud, J.M. Marechal, Y. Lasne, Differential RNA expression of the PS2 gene in the human benign and malignant prostate tissue, J. Urol. 162 (1999) 927–930.

[18] H. Sasano, H. Nagura, S.G. Silverberg, Immunolocalization of c-myc oncoprotein in mucinous and serous adenocarcinomas of the ovary, Hum. Pathol. 23 (1992) 491–495.

[19] T. Suzuki, H. Sasano, H. Aoki, H. Nagura, N. Sasano, T. Sano, et al., Immunohistochemical comparison between anaplastic seminoma and typical seminoma, Acta Pathol. Jpn 43 (1993) 751–757.

[20] T. Suzuki, T. Nakata, Y. Miki, C. Kaneko, T. Moriya, T. Ishida, et al., Estrogen sulfotransferase and steroid sulfatase in human breast carcinoma, Cancer Res. 63 (2003) 2762–2770.

[21] S. Shibahara, M. Yoshizawa, H. Suzuki, K. Takeda, K. Meguro, K. Endo, Functional analysis of cDNAs for two types of human hem oxygenase and evidence for their separate regulation., J. Biochem. (Tokyo) 113 (1993) 214–218.

[22] B.C. Lewis, H. Shim, Q. Li, C.S. Wu, L.A. Lee, A. Maity, C.V. Dang, Identification of putative c-*myc*-responsive genes: characterization of *rcl*, a novel growth-related gene, Mol. Cell Biol. 17 (1997) 4967–4978.

[23] C.V. Ramana, N. Grammatikakis, M. Chernov, H. Nguyen, K.C. Goh, B.R.G. Williams, G.R. Stark, Regulation of c-*myc* expression by IFN-γ through Stat1-dependent and -independent pathways, Eur. Mol. Biol. Org. J. 19 (2000) 263–272.

[24] I.D. Xynos, A.J. Edgar, L.D.K. Buttery, L.L. Hench, J.M. Polak, Gene-expression profiling of human osteoblasts following treatment with the ionic products of Bioglasst 45S5 dissolution, J. Biomed. Mater. Res. 55 (2001) 151–157.

[25] M.M. Partlin, E. Homer, H. Robinson, C.J. McCormick, D.H. Crouch, S.T. Durant, et al., Interactions of the DNA mismatch repair proteins MLH1 and MSH2 with c-MYC and MAX, Oncogene 22 (2003) 819–825.

[26] X. Zhang, W.J. Hendry III, Neonatal diethylstilbestrol treatment alter the estrogen-regulated expression of both cell proliferation and apoptosis-related proto-oncogenes (c-*jun*, c-*fos*, c-*myc*, *bax*, *bcl*-2, and *bcl-x*) in the hamster uterus, Cell Growth Differ. 8 (1997) 425–434.

[27] F.S. Campbell, E. Napke, N.Z. Mikhael, H.S. Buttar, A. Berzowski, L. Tryphonas, et al., Iatrogenic disease of the female genital tract in: H. Fox, M. Wells et al. (Eds.), Haines and Taylor Obstetrical and Gynaecological Pathology fourth ed., Churchill Livingstone, New York, 1995, pp. 1183–1208.

[28] G.I. Gorodeski, Estrogen increases the permeability of the cultured human cervical epithelium by modulating cell deformability, Am. J. Physiol. 275 (1998) C888–C899.

[29] T. Okubo, Y. Yokoyama, K. Kano, I. Kano, ER-dependent estrogenic activity of parabens assessed by proliferation of human breast cancer MCF-7 cells and expression of ERα and PR, Food Chem. Toxicol. 39 (2001) 1225–1232.

[30] A. Okada, T. Sato, Y. Ohta, D.L. Buchanan, T. Iguchi, Effect of diethylstilbestrol on cell proliferation and expression of epidermal growth factor in the developing female rat reproductive, J. Endocrinol. 170 (2001) 539–554.

[31] J.F. Couse, D. Dixon, M. Yates, A.B. Moor, L. Ma, R. Maas, K.S. Korach, Estrogen receptor a knockout mice exhibit resistance to the developmental effects on neonatal diethylstilbestrol exposure on the female reproductive tract, Dev. Biol. 238 (2001) 224–238.

[32] J. Takeyama, T. Suzuki, S. Inoue, C. Kaneko, H. Nagura, N. Harada, H. Sasano, Expression and cellular localization of estrogen receptor a and b in the human fetus, J. Clin. Endcrinol. Metab. 86 (2001) 2258–2262.

[33] G. Riou, M. Barrois, M.G. Le, M. George, V. LeDoussal, C. Haie, C-myc proto-oncogene expression and prognosis in early carcinoma of the uterine cervix, Lancet I (1987) 761–763.

[34] A.J. Obaya, M.K. Mateyak, J.M. Sedivy, Mysterious liaisons: the relationship between c-Myc and the cell cycle, Oncogene 18 (1999) 2934–2941.